

Synthesis and Characterization of Derivatives of the Antifungal Peptoid RMG8-8

Erin J. Pratt, Elena I. Mancera-Andrade, and Kevin L. Bicker*

Cite This: *ACS Omega* 2022, 7, 36663–36671

Read Online

ACCESS |



Metrics & More

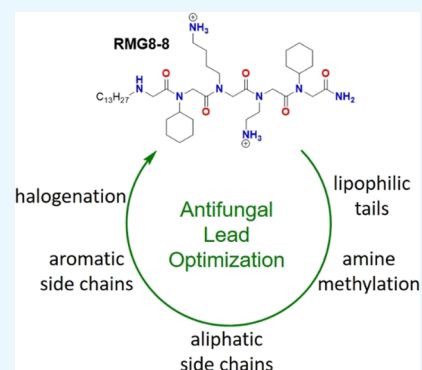


Article Recommendations



Supporting Information

ABSTRACT: Cryptococcal meningitis, caused by the fungal pathogen *Cryptococcus neoformans*, is a devastating disease with a mortality rate of over 80%. Due to the increasing prevalence of resistance to antifungals and the high mammalian toxicity of current treatments, the development of new antifungal therapies is vital. In an effort to improve the biological properties of a previously discovered antifungal peptoid, termed RMG8-8, an iterative structure–activity relationship study was conducted. This three-round study sought to optimize the structure of RMG8-8 by focusing on three main structural components: the lipophilic tail, aliphatic side chains, and aromatic side chains. In addition to antifungal testing against *C. neoformans*, cytotoxicity testing was also performed on all derivatives against human liver cells, and select promising compounds were tested for hemolytic activity against human red blood cells. A number of derivatives containing unique aliphatic or aromatic side chains had antifungal activity similar to RMG8-8 (MIC = 1.56 $\mu\text{g}/\text{mL}$), but all of these compounds were more toxic than RMG8-8. While no derivative was improved across all biological tests, modest improvements were made to the hemolytic activity with compound 9, containing isobutyl side chains in positions 2 and 5, compared to RMG8-8 (HC₁₀ = 130 and 75 $\mu\text{g}/\text{mL}$, respectively). While this study did not yield a dramatically optimized RMG8-8 derivative, this result was not totally unexpected given the remarkable selectivity of this compound from discovery. Nonetheless, this study is an important step in the development of RMG8-8 as a viable antifungal therapeutic.



INTRODUCTION

Microorganisms such as fungi are ubiquitous in the environment and, while most are innocuous, others display pathogenicity. *Cryptococcus neoformans* is a fungal pathogen that is found in the environment such as in soil and water due to bird droppings. It can enter the body through respiration and cause a pulmonary infection called cryptococcosis in immunocompromised individuals.¹ *C. neoformans* has a polysaccharide capsule that surrounds the cell membrane and contributes to its high virulence because it evades phagocytosis by immune cells.^{2,3} The organism can shed large amounts of capsular material into the body that can facilitate spread to other susceptible areas such as the central nervous system.³ Hence, the impact on an immunocompromised individual is even more severe. As *C. neoformans* infiltrates the central nervous system, an infection of the meninges called cryptococcal meningitis (CM) can occur.⁴ CM affects almost 1 million people worldwide and causes several hundred thousand deaths per year.⁵ While CM is a worldwide disease, low-income and middle-income countries take the brunt of the impact.⁵ Human immunodeficiency virus and acquired immunodeficiency syndrome (AIDS) are the most common precursors to cryptococcal infections, with around 15–20% of AIDS-related deaths being caused by cryptococcosis.^{5,6}

Fungi are eukaryotes; therefore, agents that are active against fungal cells tend also to be active against host cells.⁷ Antifungal

agents such as fluconazole, flucytosine, and amphotericin B (AmpB) are currently available to treat fungal infections caused by *C. neoformans*, and while these can be potent against fungal infections, they are known to have worrisome mammalian cytotoxicity, with up to 50% of recipients experiencing acute renal failure when treated with AmpB.^{8,9} Due to the high mammalian toxicity of AmpB, it is only administered in cases of severe systemic infections such as CM. Flucytosine is often administered together with AmpB, though it is extremely toxic to mammalian cells and has insufficient uptake by fungal cells.¹⁰ Even though flucytosine is characterized by gastrointestinal and hepatic toxicity, it is still one of the most effective antifungals on the market. While fluconazole is significantly less toxic than AmpB and flucytosine, it is not as effective for broad spectrum treatment and has up to a 20% relapse rate when used as a monotherapy.^{9,11} Because of this, it is most often administered after initial treatment with other more potent drugs and serves

Received: July 28, 2022

Accepted: September 26, 2022

Published: October 4, 2022



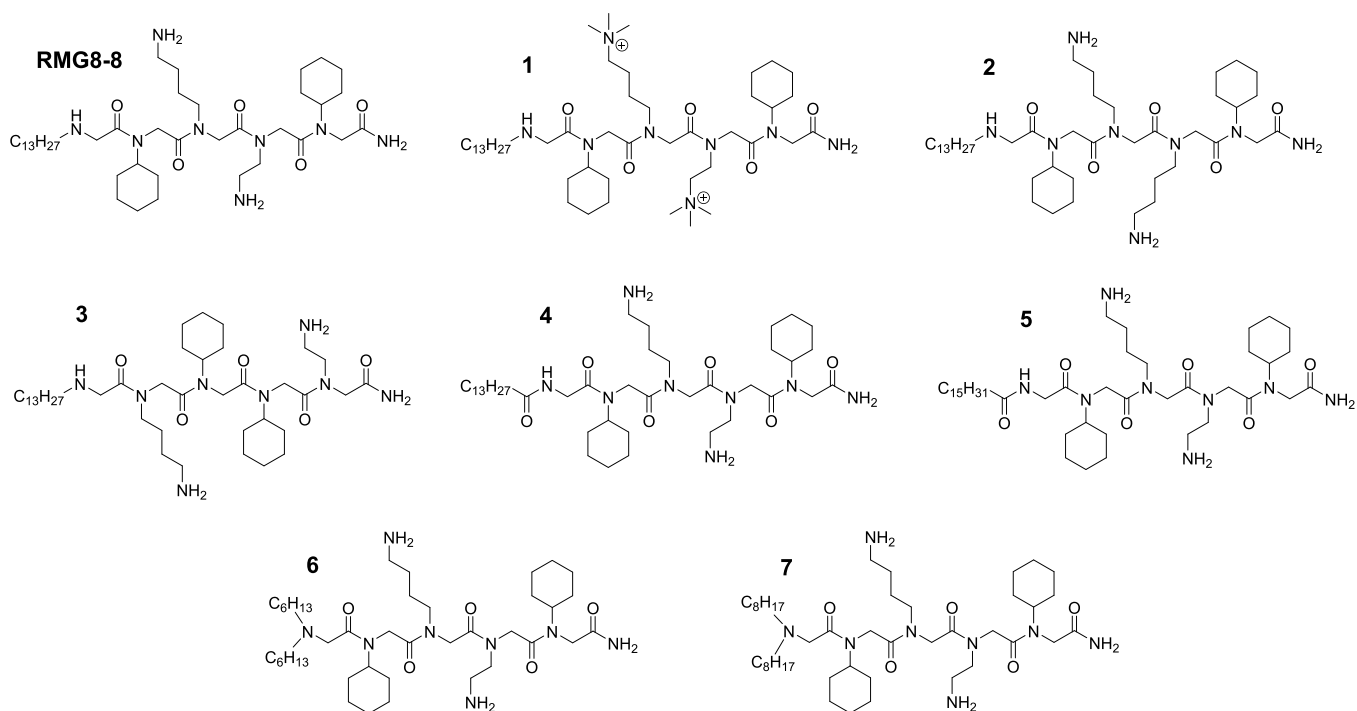


Figure 1. Structure of lead compound RMG8-8 and round 1 derivatives, including miscellaneous modifications that have proven useful in past studies and variations in the lipophilic tail.

best as a maintenance or prophylactic therapy.⁸ As a whole, treatment for infections like CM can be prolonged, leaving affected individuals at the mercy of maintenance therapy for several months to years.⁸

New therapies have made great progress in combating microbial infections; however, many pathogens have developed resistance to current treatments. Antimicrobial resistance (AMR) has put pressure on the medical community to discover and create new therapies to combat these infectious agents. Pathogenic bacteria and fungi have developed mechanisms, both transient and heritable, that render antimicrobial therapies ineffective.¹² Studies have shown *C. neoformans* to be resistant when presented with high concentrations of fluconazole requiring treatment with a combination therapy of fluconazole and flucytosine.¹³ Additionally, some *C. neoformans* strains produce enlarged capsules, known as titan cells, when infecting the lungs and have shown resistance to AmpB.¹³

The scientific community has extensively looked at naturally occurring compounds to emulate the development of modern pharmaceuticals, one such group being antimicrobial peptides (AMPs). These ubiquitous compounds were first discovered almost 100 years ago by Alexander Fleming.¹⁴ AMPs are a part of the human body's innate immune system, and therefore, they have low toxicity and continue to be widely studied by many. Generally, they are composed of cationic residues as well as hydrophobic areas, creating an overall amphipathic structure.¹⁴ Due to AMP's cationic nature, they bind to the anionic membranes of microbes and work to eliminate pathogens through membrane disruption mechanisms such as pore formation.¹⁵ While AMPs hold promise as potential antimicrobial agents, they have shortcomings, which prevent them from clinical use. AMPs are quickly recognized and eliminated by degradative proteolytic enzymes in the body, giving them a short in vivo half-life, averaging under an

hour.^{16,17} This property, combined with poor bioavailability, makes AMPs a challenging platform for the development of clinical antimicrobial agents.

The use of peptidomimetics is one way to overcome the inadequacies of AMPs. N-substituted oligoglycines, or peptoids, place the side chain on the nitrogen of the amide backbone instead of on the α -carbon. Due to this unique structure, peptoids are not recognized by proteases and have better in vivo stability than their peptide counterparts, while demonstrating low toxicity both in vitro and in vivo.^{17–22} Since the first demonstration of peptoid antimicrobial activity over 20 years ago,²³ antimicrobial peptoids have been developed against numerous bacteria, fungi, parasites, and viruses.^{24,25} Promising antimicrobial peptoids have been developed with activity against the ESKAPE bacteria,^{16,17,26–32} *Mycobacterium tuberculosis*,³³ fungi, including *Cryptococcus neoformans*, *Candida albicans*, and *Candida auris*,^{22,34–39} and viruses, including HSV-1 and SARS-CoV-2.⁴⁰

Design, synthesis, and screening of potentially effective antimicrobial peptoids is a tedious endeavor, and so, combinatorial libraries and high-throughput screening methods are essential for quick identification. The Peptoid Library Agar Diffusion (PLAD) assay has been developed to interrogate combinatorial peptoid libraries to identify compounds with promising antimicrobial activity.^{35,37,41} One particular PLAD screening against *C. albicans* led to the discovery of a peptoid with moderate activity against *C. albicans*, termed RMG8-8 (Figure 1).³⁵ With a minimum inhibitory concentration (MIC) of 25 $\mu\text{g}/\text{mL}$ and low mammalian cytotoxicity against human liver cells ($\text{TD}_{50} = 189 \mu\text{g}/\text{mL}$), RMG8-8 was characterized further. While only moderately active against *C. albicans*, proved to be highly active against *C. neoformans* with an MIC of 1.56 $\mu\text{g}/\text{mL}$, which is more potent than fluconazole or flucytosine.⁴² Further characterization indicated that RMG8-8 killed fungi rapidly ($t_{1/2} = 6.5 \text{ min}$), was proteolytically stable,

and likely exerted antifungal activity through membrane disruption.³⁵

The natural next step after discovery of any promising lead compound is structure modification to improve biological activity. Structure–activity relationship (SAR) studies in peptoids utilize iterative design to modify structures and can be helpful in determining the pharmacological significance of each peptoid monomer.²¹ One method used to determine each monomer's role in overall biological activity is called a sarcosine scan. Sarcosine is *N*-methylglycine, and therefore, a sarcosine scan in peptoids is equivalent to an alanine scan in peptides.⁴³ Each monomer of a peptoid is replaced one at a time with a sarcosine to determine the effect of a single residue on the overall pharmacological activity of a compound. This type of sarcosine scan was previously done with the antifungal peptoid AEC5.³⁶ The ensuing modular SAR study of AEC5, where monomers were optimized in order of their pharmacological importance with the optimized monomer carried forward into subsequent rounds, yielded the peptoid β -5 with increased antifungal activity and decreased toxicity relative to the lead compound, AEC5.³⁶

The sarcosine scan for RMG8-8 was completed shortly after discovery and initial characterization, revealing the lipophilic tail of RMG8-8 to be most pharmacologically important, followed by the cyclohexyl groups, followed by the cationic moieties, which were primarily responsible for mitigating cytotoxicity.³⁵ Here, we report the attempted optimization of RMG8-8 through an iterative SAR study against *C. neoformans*. A three-round modular SAR study yielded 25 different compounds for analysis containing various lipophilic tails, aliphatic and aromatic substitutions of the cyclohexyl groups, and trimethylation of the cationic amino side chains. Ultimately, none of the compounds tested had improved overall biological activity, as determined by the selectivity ratio (SR) for *C. neoformans* over liver cells, compared with RMG8-8. Even with this result, this study is an important and necessary step in the development of RMG8-8 toward the treatment of deadly fungal infections.

RESULTS AND DISCUSSION

All RMG8-8 derivatives were synthesized via the solid-phase submonomer synthesis method on polystyrene Rink Amide resin.⁴⁴ The amines used during synthesis and the peptoid shorthand notations for each monomer are provided in Tables S1 and S2, respectively. Compounds were purified to greater than 95% by RP-HPLC and compound identity was confirmed by electrospray ionization time-of-flight mass spectrometry (ESI-TOF MS, Table S3 and Figures S1–S25). The calculated distribution coefficient at pH 7.4 ($c\text{Log}D_{7.4}$)⁴⁵ and the percent acetonitrile at the time of elution during HPLC purification were recorded and serve as measures of hydrophobicity (Table 1). Higher values for $c\text{Log}D_{7.4}$ and percent acetonitrile are indicators of increased compound hydrophobicity. With antimicrobial peptoids, hydrophobicity is directly related to both antimicrobial activity and cytotoxicity.^{46–48} The ideal balance of these parameters generally must be determined experimentally. To measure antifungal activity, the MIC, defined as the concentration of compound required to inhibit 90% of fungal growth, was determined against *C. neoformans* using the broth microdilution method. Mammalian cytotoxicity was evaluated through a cell metabolic activity assay with HepG2 liver carcinoma cells, and select, potentially promising

Table 1. Physicochemical and Biological Characterization of Antifungal Peptoids

compound	$c\text{Log}D_{7.4}$	% ACN	<i>C. neoformans</i> MIC ($\mu\text{g}/\text{mL}$)	HepG2 TD ₅₀ ($\mu\text{g}/\text{mL}$)	selectivity ratio
RMG8-8 ^a	−2.38	70.0%	1.56	189 ± 43	121
1	−5.22	73.3%	12.5	>200	ND
2	−2.74	67.4%	3.13	165 ± 97	53
3	−2.38	69.3%	3.13	105 ± 3.8	34
4	−1.34	73.7%	6.25	>200	ND
5	−0.45	80.1%	3.13	85 ± 16	27
6	−2.53	64.5%	100	>200	ND
7	−0.75	69.3%	6.25	162 ± 29	26
8	−4.43	66.7%	25	>200	ND
9	−3.49	68.1%	3.13	167 ± 75	53
10	−1.55	73.3%	1.56–3.13	61 ± 9	19–39
11	−3.27	68.1%	6.25	>200	ND
12	−1.75	71.4%	1.56–3.13	62 ± 3	20–40
13	−5.14	67.3%	12.5–25	>200	ND
14	−2.36	67.7%	1.56–3.13	81 ± 25	26–52
15	−2.53	66.9%	1.56–3.13	145 ± 96	46–93
16	−1.7	66.7%	1.56–3.13	167 ± 104	53–107
17	−2.24	69.3%	1.56–3.13	150 ± 7	48–96
18	−1.32	71.1%	3.13	72 ± 24	23
19	−0.99	72.3%	3.13	72 ± 20	23
20	−0.67	72.1%	6.25	72 ± 24	12
21	−0.36	71.1%	6.25	118 ± 19	19
22	−0.35	71.5%	1.56–3.13	91 ± 4	29–58
23	−2.37	69.9%	1.56–3.13	85 ± 10	27–54
24	−4.41	67.6%	3.13–6.25	143 ± 94	23–46
25	−2.7	68.3%	1.56–3.13	154 ± 47	49–99

^aRMG8-8 parameters from previously published results.³⁵ Calculated distribution coefficients at pH 7.4 ($c\text{Log}D_{7.4}$) from MarvinSketch.⁴⁵ All assays were run in triplicate, and standard deviation is provided with HepG2 toxicity values. The SR was calculated by dividing the toxicity (TD₅₀) by the antifungal activity (MIC). % ACN, percent acetonitrile at the time of elution from HPLC; MIC, minimum inhibitory concentration; TD₅₀, toxicity dose 50%; ND, not done, Rounds 1, 2, and 3 include compounds 1 to 7, 8 to 13, and 14 to 25, respectively.

compounds were tested for unwanted hemolytic activity against human red blood cells (hRBCs).

Round 1 of the modular SAR included miscellaneous alterations that have proven beneficial in past studies and modifications to the lipophilic tail in position 1, which is the most pharmacologically important monomer (Figure 1).³⁵ Miscellaneous alterations include trimethylation of the side chain amines (1), substitution of the Nae monomer with Nlys (2), and rearrangement of the RMG8-8 sequence (3). Trimethylation of side chain amines was done to lock in the cationic charge, which was hypothesized would decrease the toxicity of the compound, consistent with a previous peptoid SAR.³⁶ Substitution of the Nae residue in position 4 to an Nlys was justified by the same previous SAR study, which indicated that the slightly longer cationic side chains had reduced mammalian cytotoxicity.³⁶ Additionally, inverting positions 2 and 5 with 3 and 4 was done to determine if the monomer order was important for biological activity. Compounds 4–7 all contained different lipophilic tails, namely myristic acid, palmitic acid, dihexylamine, and dioctylamine, respectively. The fatty acid derivatives were explored because previous studies demonstrated that lipopeptides with fatty acid

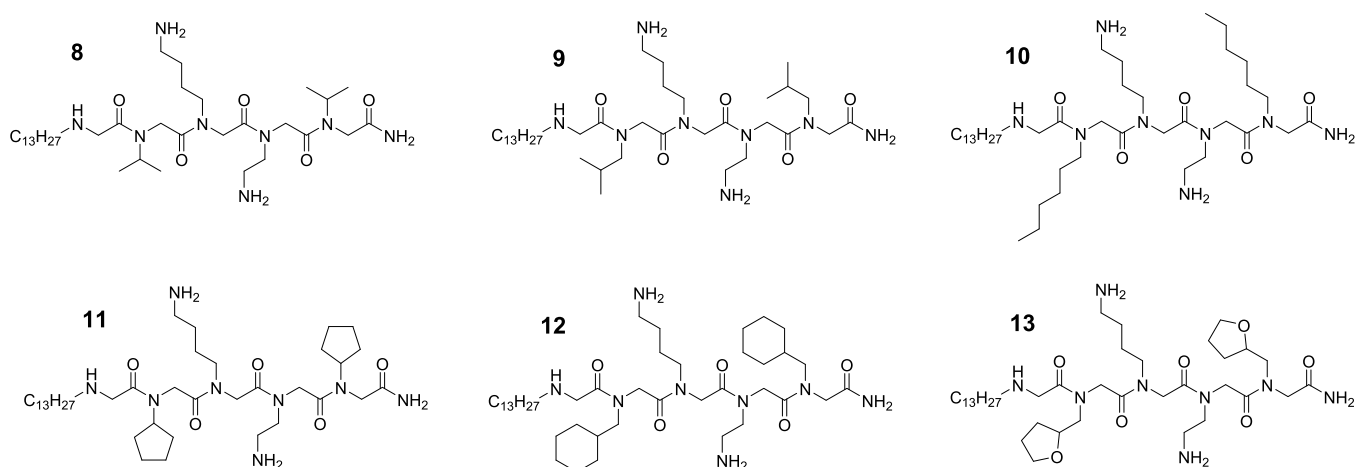


Figure 2. Structure of round 2 derivatives, substituting various aliphatic side chains into positions 2 and 5.

tails were less toxic than those with aliphatic amine tails.¹⁶ The double tails in compounds **6** and **7** were hypothesized to potentially increase potency as they could provide more interactions with the fungal membrane than a single tail and could potentially cause more fungal cell membrane disruption.

Physicochemical measurements indicated that within the first round of compounds, compound **1** would be the most hydrophilic owing to the locked cations, while compound **5** with the 16-carbon palmitic acid tail and compound **7** with the dioctyl tail would be the most hydrophobic (Table 1). The broth microdilution method provided a measure of antifungal activity as MIC, and cytotoxicity was determined against HepG2 cells and calculated as the concentration of the compound resulting in 50% inhibition of viable cells, termed the toxicity dose 50% or TD₅₀. The SR was calculated by dividing toxicity (TD₅₀) by potency (MIC) and was used to obtain a picture of the overall therapeutic window of a compound (Table 1). While trimethylated compound **1** did in fact reduce cytotoxicity beyond the highest concentration tested (>200 μg/mL), the antifungal activity decreased eightfold, indicating that trimethylation was not a useful strategy for improving RMG8-8. Compound **2** displayed a twofold loss in activity and an insignificant change in cytotoxicity, indicating that the length of the diamine used is inconsequential. Compound **3**, which contained the same monomers as RMG8-8 but in a different order, showed a twofold decrease in MIC against *C. neoformans* and a modest increase in cytotoxicity. It is interesting to observe and note the effect of the monomer order on cytotoxicity, though the reason for this effect is unknown. Compound **4**, though more hydrophobic than RMG8-8, displayed decreased cytotoxicity, consistent with previous studies exploring fatty acid tails,¹⁶ but also had weakened antifungal activity. The longer fatty acid tail-modified compound **5** had improved antifungal activity compared to compound **4** but was still diminished compared to RMG8-8. Additionally, the cytotoxicity for compound **5** was the greatest for any compound tested in round 1. Though the calculated hydrophobicity for compound **6** was similar to RMG8-8, compound **6** displayed a dramatic loss in antifungal activity, with an MIC of 100 μg/mL, likely due to the short six-carbon chains. This indicates that the antifungal activity of lipopeptides containing long aliphatic tails, such as those tested here and by others, is not necessarily due to the overall hydrophobicity provided by that tail but more importantly to

how the length of the tail disrupts microbial membranes. Compound **7**, with dioctyl tails, also had diminished antifungal activity and comparable cytotoxicity compared to RMG8-8. Overall, round 1 explored a number of previously valuable modifications and uniquely new tail modifications but did not yield a compound with improved activity or selectivity compared to RMG8-8.

Since it was confirmed that the tridecylamine tail in position 1 was the optimal option, this was carried over to all derivatives in round 2. Round 2 explored various aliphatic side chain derivatives in positions 2 and 5 simultaneously since these positions are identical in RMG8-8 and had identical results when substituted with sarcosine (Figure 2).³⁵ These side chains were chosen to explore multiple parameters including size, cyclic versus acyclic, and heterocyclic effects. Compounds **8** and **9** contained smaller isopropyl and isobutyl groups, respectively, which were hypothesized to decrease overall hydrophobicity and toxicity. Compound **10** contained a straight chain hexyl group instead of the cyclohexyl group found in RMG8-8. Compounds **11** and **12** contained cyclopentyl and cyclohexylmethyl groups, respectively, rationalizing that the cyclic nature of the side chains in these positions could be important but optimizable. Lastly, compound **13** explored a heterocycle by incorporating a tetrahydrofurfuryl group.

Physicochemical analysis indicated that in round 2, compound **10** containing straight chain hexyl groups was the most hydrophobic and significantly more hydrophobic than RMG8-8 containing cyclohexyl groups (Table 1). Compounds **8** and **13** were the least hydrophobic, as the isopropyl and tetrahydrofuran moieties of each compound reduced the number of methylenes and added a heteroatom, respectively. Biological characterization indicated that compounds **10** and **12** retained antifungal activity similar to RMG8-8, but with markedly higher cytotoxicity, giving poor SRs (Table 1). Both of these compounds demonstrate the structural nuance that affects biological activity and highlight the challenge of lead peptoid optimization. Compound **10** only differs in the cyclic nature of the hexyl side chain and compound **12** only differs in the addition of a methylene between the amide backbone and the side chain; however, these properties are critical for the excellent selectivity of RMG8-8. Compounds **8**, **11**, and **13**, all with low hydrophobicity compared to RMG8-8, had cytotoxicity values greater than 200 μg/mL. However, each

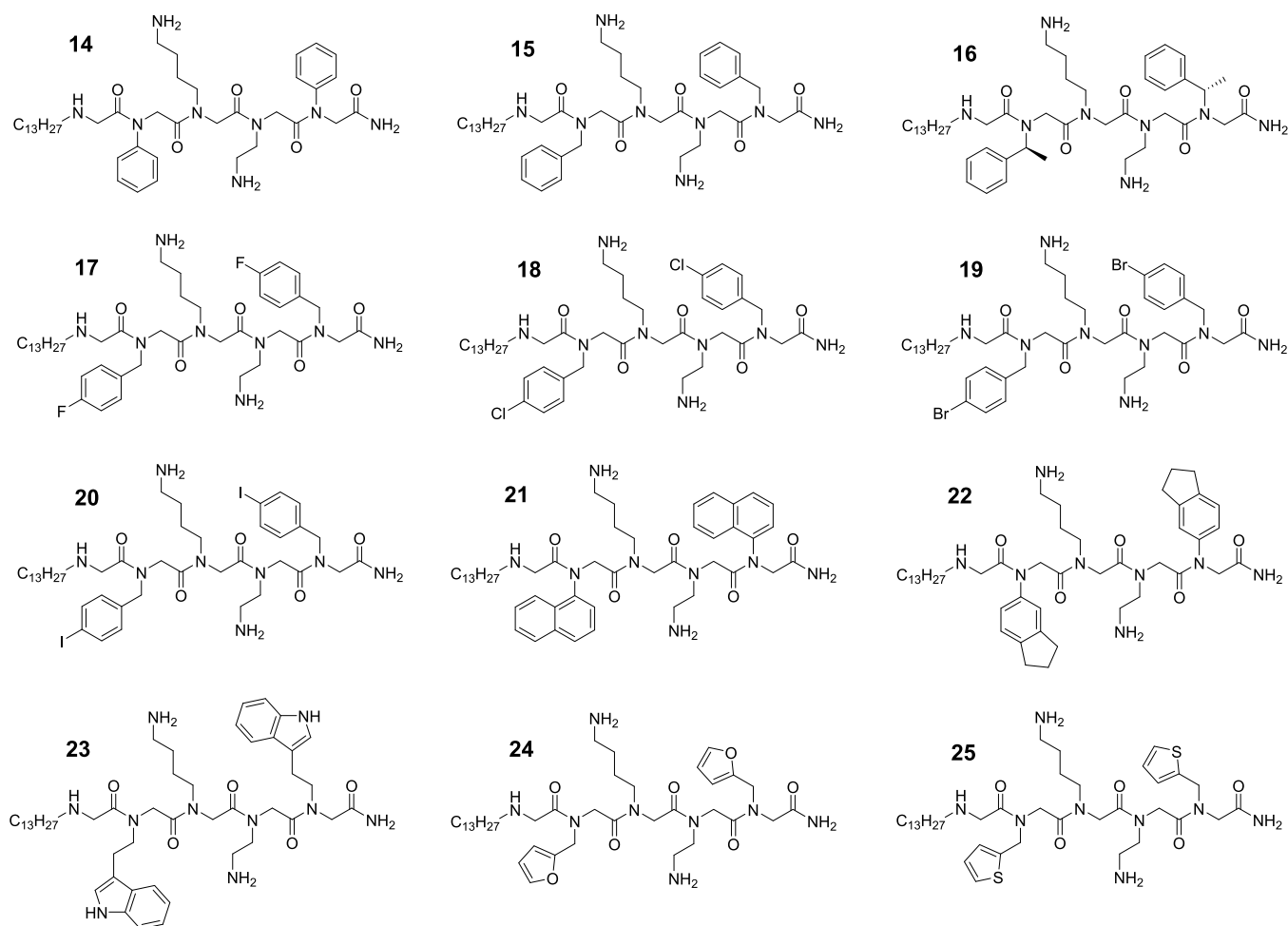


Figure 3. Structure of round 3 derivatives, substituting various aromatic side chains into positions 2 and 5.

of these compounds also displayed 4- to 16-fold decreases in antifungal efficacy. Compound 9 with isobutyl side chains was the most promising with only twofold diminished antifungal activity and modest cytotoxicity; however, this compound still fell well short of the SR of RMG8-8. Ultimately, no round 2 derivative displayed improved biological selectivity compared to RMG8-8, and therefore, Round 3 was designed to next explore aromatic side chain derivatives.

Round 3 was the largest round, with 12 compounds consisting of aromatic derivatives in positions 2 and 5 (Figure 3). Simpler aromatic side chains were chosen first for compounds 14, 15, and 16, containing phenyl, benzyl, and (*S*)-methylbenzyl side chains, respectively. The (*S*)-methylbenzyl side chain is popular and prevalent among previously explored antimicrobial peptoids.²⁵ Halogenated aromatics were also explored in compounds 17, 18, 19, and 20 containing para fluoro, chloro, bromo, and iodo benzyl side chains, respectively. Halogenated side chains have proven useful in optimizing antibacterial activity and selectivity in a previous study.⁴⁹ Fused ring systems were explored in compounds 21 and 22, incorporating naphthyl and indanyl side chains, respectively. Lastly, aromatic heterocycles were explored in compounds 23, 24, and 25 incorporating indolylethyl, furylmethyl, and thiophenylmethyl side chains, respectively. The furylmethyl and thiophenylmethyl side chains have proven useful in previous antifungal peptoids.^{34,36,37}

Physicochemical analysis indicated that derivatives containing large halogens (19 and 20) or fused ring systems (21 and 22) were the most hydrophobic (Table 1). Unsurprisingly, compounds containing heteroaromatic side chains (24 and 25) were the least hydrophobic. The addition of aromatic moieties increased antifungal activity as a whole compared to previous modifications (Table 1). This can most likely be attributed to an increase in membrane disruption due to the larger, more hydrophobic groups in positions 2 and 5. However, while some compounds had similar efficacy compared to RMG8-8, none performed better than this lead peptoid. One disadvantage of bulkier, more hydrophobic side chains is the increase in mammalian cytotoxicity. Compounds 14, 18, 19, 20, 21, 22, and 23 displayed disqualifying cytotoxicity, with TD_{50} values well below the TD_{50} of $189 \pm 43 \mu\text{g/mL}$ for RMG8-8. Compounds containing the benzyl (15), methylbenzyl (16), or para-fluorobenzyl (17) side chain showed cytotoxicity similar to RMG8-8. Likewise, compounds 24 and 25 containing aromatic heterocycles had only modestly lower SRs compared to RMG8-8. Interestingly, increasing halogen size resulted in decreased antifungal activity, which is contrary to previously published work on antibacterial peptoids.⁴⁹ It is possible that antimicrobial trends related to halogenated peptoids are dissimilar when targeting bacteria versus fungi, though more detailed analysis would be required to firmly conclude this.

While none of the SAR derivatives tested here were more active and less toxic than RMG8-8, select compounds had only

slightly diminished SRs. As a further important measure of mammalian cytotoxicity, these select compounds (**9**, **16**, **17**, and **25**) were tested for hemolytic activity against hRBCs. An unwanted result of certain medications, hemolysis is the breakdown or lysis of red blood cells and is an important indicator of toxicity.⁵⁰ Red blood cells come from primary donors and are not immortally cultured like HepG2 cells, and therefore, hemolysis can vary from donor to donor. Therefore, RMG8-8 was reevaluated along with the selected derivatives against the same donor sample of hRBCs (Table 2). Of these

Table 2. Hemolysis Analysis for Select Compounds against Human Red Blood Cells (hRBCs)^a

compound	hRBC HC ₁₀ (μg/mL)	selectivity ratio
RMG8-8	75 ± 31	48
9	130 ± 45	42
16	38 ± 11	12–24
17	59 ± 22	19–38
25	81 ± 37	26–52

^aHemolysis reported as the concentration of compound resulting in 10% hemolysis (HC₁₀). All assays were run in triplicate and standard deviation is provided. Selectivity ratio is calculated by dividing the HC₁₀ by the antifungal activity (MIC). HC₁₀, hemolytic concentration 10%.

peptoids, compound **9** (HC₁₀ = 130 ± 45 μg/mL) showed promising results as it was significantly less hemolytic than RMG8-8 (HC₁₀ = 75 ± 31 μg/mL). Compound **25** displayed comparable hemolytic activity, and compounds **16** and **17** were markedly more hemolytic than RMG8-8. The decrease in hemolysis between compound **9** and RMG8-8 is most likely attributed to the overall decrease in hydrophobicity with the isobutyl side chains in compound **9**, as seen in previous studies.^{16,50} While the decreased hemolytic activity of compound **9** is encouraging, none of the compounds tested here had significantly increased SRs compared to RMG8-8.

CONCLUSIONS

The goal of this research was to optimize the lead antifungal peptoid, RMG8-8, via an iterative SAR study. A three-round SAR was executed, with each round utilizing a different strategy of modification. Round 1 consisted of lipophilic tail derivatives in position 1 and other miscellaneous alterations that had previously shown promise. Round 2 included varying aliphatic residues in positions 2 and 5 and round 3 contained aromatic derivatives in these same positions. Altogether, the derivatives synthesized here explored a diversity of chemical space to try and identify modifications that could improve the biological activity of RMG8-8. The improved hemolytic activity with compound **9** is important and this compound had MIC and cytotoxicity values comparable to those of RMG8-8, meriting continued evaluation of this peptoid. Ultimately though, this study did not yield a peptoid with dramatically improved biological properties compared to RMG8-8. However, this acknowledges the power of the PLAD assay, which discovered RMG8-8 to interrogate large amounts of chemical space to identify peptoids, which already possess promising biological properties. The development of RMG8-8 as a viable antifungal therapeutic is ongoing, with current efforts focused on in vivo characterization of pharmacological and efficacy properties.

METHODS

Materials. All reagents were purchased at greater than 95% purity. Reagents and materials were purchased from Fisher Scientific (Waltham, MA), Alfa Aesar (Haverhill, MA), TCI America (Portland, OR), Amresco (Solon, OH), EMD Millipore (Billerica, MA), Supra Sciences (Belmont, CA), Corning (Tewksbury, MA), and Chem-Impex (Wood Dale, IL). Mono-methoxytrityl-protected diamines were synthesized as previously described.¹ hRBCs were acquired from Innovative Research (Novi, MI). All mass spectra were acquired on a Waters Synapt HDMS QToF with Ion Mobility. Purification of compounds was achieved using a Varian Prepstar SD-1 with a Supelco Ascentis C18 column (5 μM; 25 cm × 21.2 mm; Sigma-Aldrich 581,347-U) and a 0–100% gradient of water to acetonitrile containing 0.05% trifluoroacetic acid (TFA). The distribution coefficient, cLogD_{7.4}, was determined using MarvinSketch.²

General Peptoid Synthesis Procedure. Peptoids were synthesized on the solid phase using the submonomer approach as previously described.³ These methods were sufficient for synthesizing most of the peptoids studied here. More unique methods required for certain peptoids are described below. Polystyrene resin with a Rink Amide linker (loading capacity: 0.75 mmol/g) was placed in a fritted column and swelled with dimethylformamide (DMF) for 30 min followed by Fmoc deprotection with 20% piperidine 2× for 10 min each. A Kaiser test was utilized to determine full Fmoc deprotection. After a DMF wash 3×, the resin was acylated with 2 M bromoacetic acid in anhydrous DMF (1.5 mL) and 3.2 M diisopropylcarbodiimide in anhydrous DMF (1.5 mL). The reaction was microwaved at 10% power for 15 s 2× and then allowed to rock for 15 min. The solution was aspirated from the resin, and the resin was washed 3× with DMF. A Kaiser test was performed to ensure that the reaction was successful. For submonomer addition, a 2 M solution of the desired amine (3 mL) was added to the resin and microwaved at 10% power for 15 s 2× and then placed on the rocker for 30 min. These alternating steps of acylation and amination were repeated with the necessary amines until the desired peptoid structure was achieved. The amines used during synthesis of each compound and the monomer shorthand codes are provided in Tables S1 and S2, respectively. The final submonomer addition for the lipophilic tail was allowed to rock overnight at 35 °C to maintain amine solubility and improve reaction yield. Resin was washed with DMF 3× and CH₂Cl₂ 3× and allowed to dry under vacuum for 5 min. To cleave the compound from the resin, a mixture of 95% TFA: 2.5% triisopropylsilane: 2.5% H₂O was added and rocked for 1 h. The reaction solution was drained from the resin into a 50 mL conical tube, and the TFA was evaporated under a stream of air. The resulting oil was reconstituted in 1:1 acetonitrile (ACN):H₂O (8 mL) in preparation for purification.

Compound 1 Synthesis. Synthesis of compound **1** followed that of the General Peptoid Synthesis Procedure until after the addition of the lipophilic tail. Following this addition, Boc protection of the N-terminal amine was achieved by treating with Boc-anhydride (430 μL; 1.87 mmol) in 5% N-methylmorpholine (NMM) in DMF (5 mL) for 1 h with rocking. The resin was washed with DMF 3× and CH₂Cl₂ 3×. To remove the Mmt protecting groups, the resin was treated 6× with 1% TFA in CH₂Cl₂ (5 mL) for 10 min each, followed by washing with CH₂Cl₂ 3× and DMF 3×.

Resin amines were free-based by treating with 5% NMM in DMF for 5 min and then trimethylated with methyl iodide (118 μL ; 1.9 mmol) and cesium carbonate (619 mg; 1.9 mmol) in DMF (5 mL), while rocking overnight at 25 $^{\circ}\text{C}$. Resin was washed with DMF 3 \times , water 3 \times , DMF 3 \times , and then CH_2Cl_2 3 \times . The compound cleavage procedure was followed, which also removed the N-terminal Boc group.

Synthesis of Compounds 4 and 5. Synthesis of compounds 4 and 5 followed that of the General Peptoid Synthesis Procedure until the addition of the aliphatic tail, which for these peptoids was a fatty acid. Fmoc-glycine-OH (222.75 mg; 0.75 mmol) was activated with 3-[bis-(dimethylamino)methylumyl]-3H-benzotriazol-1-oxide hexafluorophosphate (HBTU, 284.4 mg; 0.75 mmol) in 5% NMM in DMF (7 mL) for 10 min. This solution was added to the resin and rocked for 1 h. After aspiration and washing with DMF 3 \times , a Kaiser test was performed to verify successful coupling. 20% piperidine in DMF was used to remove Fmoc-protecting groups (~ 7 mL 2 \times for 10 min each). Another Kaiser test was performed to confirm the removal of Fmoc. 4 molar equiv of myristic acid (compound 4) and palmitic acid (compound 5) were activated with HBTU (284.4 mg; 0.75 mmol) in 5% NMM in DMF for 10 min. This solution was added to the resin and rocked for 1 h. After aspiration, a DMF wash was performed 3 \times , and a Kaiser test was used to confirm proper coupling. The resin was then washed with CH_2Cl_2 3 \times and allowed to dry for 5 min under vacuum. The compound cleavage procedure was then followed.

Purification. Peptoids were purified to greater than 95% via reverse-phase high-performance liquid chromatography (RP-HPLC) using a Varian Prepstar SD-1. A gradient of 0–100% water to acetonitrile containing 0.05% TFA made up the mobile phase, and a Supelco Ascentis C18 column (5 μm ; 25 cm \times 21.2 mm; Sigma-Aldrich 581347-U) was used as the stationary phase. Peaks in the chromatogram above 0.1 AU were collected and analyzed via mass spectrometry. The peak product with the desired peptoid was dried down *in vacuo* and lyophilized overnight. Peptoids were then reconstituted in sterile 18 m Ω deionized water to create compound stocks of 20 mg/mL.

MS Analysis. Compounds were analyzed with ESI-TOF MS via Waters Synapt HDMS. For analysis of RP-HPLC purified products, the collected peaks were directly injected into the mass spectrometer and presence of the compounds' mass/charge was verified (Figures S1–S25).

MIC Determination. MIC assays against *C. neoformans* were carried out following CLSI guidelines as described previously.^{4,5} YPD agar plates were streaked with *C. neoformans* frozen culture stock and incubated for 72 h at 35 $^{\circ}\text{C}$. After incubation, a sterile loop was used to transfer 1–2 colonies to 5 mL of 0.85% saline. After vortexing for 30 s, the optical density at 600 nm was determined by a spectrophotometer with the desired range of 0.15–0.25. The addition of 0.1 mL cell solution to 9.9 mL of RPMI-MOPS produced a 1:100 cell solution. After vortexing, 0.5 mL of the 1:100 solution was added to 9.5 mL of RPMI-MOPS to produce a 1:20 cell solution. 198 μL of the 1:20 solution was added to the wells of an opaque 96-well plate, apart from the wells designated for the medial control. Compound stocks of 20 mg/mL were used to prepare two-fold serial dilutions, and 2 μL of each compound dilution was plated in triplicate, giving final concentrations of 200, 100, 50, 25, 12.5, 6.25, 3.13, and 1.56 $\mu\text{g}/\text{mL}$. AmpB was used as a positive control, and sterile water was used for the

vehicle control. The plates were incubated for 72 h at 35 $^{\circ}\text{C}$. After incubation, the concentration of the compound resulting in no visual growth was recorded as the MIC. All assays were performed in biological triplicate on different days.

Mammalian Cytotoxicity Assay. Cytotoxicity against HepG2 hepatocellular carcinoma cells was done as previously described.^{5,6} HepG2 cells were maintained in culture in T-75 flasks using Dulbecco's Modified Eagle's Media (DMEM) with phenol red pH indicator and supplemented with 10% fetal bovine serum (FBS) and 1% penicillin, streptomycin, and glutamine. The cells were incubated at 37 $^{\circ}\text{C}$ and 5% CO_2 in a humidified incubator until desired confluency was achieved. The media was removed from the flask, and the cells were washed 1 \times with 10 mL of phosphate-buffered saline (PBS; 11.8 mM phosphate, 140.4 mM NaCl; pH 7.4), which was then discarded. To remove the adhered cells from the flask, 2 mL of trypsin was added, and the cells were incubated for 10 min. To quench the trypsin, 8 mL of phenol red-free DMEM with 10% FBS and 1% PGS was added, and the cell solution was transferred to a 15 mL conical tube. After the cells were pelleted by centrifugation at 1000 rpm for 5 min, the supernatant was poured off and cells resuspended in the volume of phenol red-free media needed for the assay. Cell concentration was determined by counting with a hemocytometer, and the solution was diluted with media until a concentration of 1×10^5 cells/mL was achieved. A 100 μL aliquot of cell solution was added to each well of a 96-well plate, apart from the 3 wells used for a media control. Cells were incubated for 2–3 h at 37 $^{\circ}\text{C}$ and 5% CO_2 until cells were adherent.

Compound stocks of 20 mg/mL were used to prepare twofold serial dilutions of each compound in sterile water, giving final concentrations of 200, 100, 50, 25, 12.5, 6.25, 3.13, and 1.56 $\mu\text{g}/\text{mL}$. 11.1 μL of the prepared compound solutions was added to the appropriate wells in triplicate. A negative vehicle control of sterile water and the aforementioned media control were used. The plates were incubated for 72 h at 37 $^{\circ}\text{C}$ and 5% CO_2 . After incubation, 20 μL of 5 mg/mL 3-(4,5-dimethylthiazol-2-yl)-2,5-diphenyltetrazolium bromide (MTT) in water was added to each well. The plate was incubated for 3 h at 37 $^{\circ}\text{C}$ and 5% CO_2 . Media was removed from each well using a sterile glass Pasteur pipette. 100 μL of DMSO was added to each well and incubated for 15 min at 37 $^{\circ}\text{C}$. Absorbance was read at 570 nm using a SpectraMax M5 Plate Reader. This MTT assay was performed in biological duplicate unless discrepant results were observed. If this was the case, the assay was performed in biological triplicate for further verification. The reported value is the average of biological replicates with standard deviation.

Hemolytic Assay. The hemolytic activity of select peptoids was determined as done previously.^{1,7} Selected peptoids were prepared in twofold serial dilutions in PBS at the desired concentrations. hRBCs (9 mL) were centrifuged at 1000 rpm for 10 min, and the supernatant was removed and discarded. A 10 mL aliquot of PBS was used to resuspend the hRBCs, which were centrifuged again at 1000 rpm for 10 min. This PBS wash was completed two more times for a total of three washes. A 9 mL aliquot of PBS was added to the hRBCs, and 100 μL of cell solution was added to individual wells of a 96-well plate. Peptoid solutions (11.1 μL) were added to the appropriate wells in triplicate. A vehicle control of PBS and positive control of 1% Triton X-100 were added to wells in triplicate.

The plate was incubated at 37 °C for 1 h and centrifuged at 1000 rpm for 10 min. For each well, 5 μ L of the supernatant was transferred to 95 μ L of PBS in a new 96-well plate. The absorbance at 405 nm was measured using a SpectraMax M5 Plate Reader, and the percent hemolysis was calculated as follows:

$$\% \text{hemolysis} = \frac{(\text{OD}_{405\text{nm}} \text{ sample} - \text{OD}_{405\text{nm}} \text{ neg. control})}{(\text{OD}_{405\text{nm}} \text{ pos. control} - \text{OD}_{405\text{nm}} \text{ sample})} \times 100$$

This hemolytic assay was performed in biological triplicate on different days.

■ ASSOCIATED CONTENT

SI Supporting Information

The Supporting Information is available free of charge at <https://pubs.acs.org/doi/10.1021/acsomega.2c04778>.

Materials, peptoid synthesis, and assay methods (PDF)

■ AUTHOR INFORMATION

Corresponding Author

Kevin L. Bicker – Department of Chemistry, Middle Tennessee State University, Murfreesboro, Tennessee 37132, United States; orcid.org/0000-0002-8638-971X;
Email: Kevin.Bicker@mtsu.edu

Authors

Erin J. Pratt – Department of Chemistry, Middle Tennessee State University, Murfreesboro, Tennessee 37132, United States

Elena I. Mancera-Andrade – Department of Chemistry, Middle Tennessee State University, Murfreesboro, Tennessee 37132, United States; orcid.org/0000-0002-0096-9650

Complete contact information is available at:
<https://pubs.acs.org/doi/10.1021/acsomega.2c04778>

Author Contributions

E.J.P. and E.I.M.-A. designed and synthesized molecules, performed compound characterization, and co-wrote the manuscript. K.L.B. helped design molecules and experiments and co-wrote the manuscript.

Notes

The authors declare no competing financial interest.

■ ACKNOWLEDGMENTS

This work was supported by the National Institutes of Health (1R03AI146393) and the Molecular Biosciences Ph.D. Program at Middle Tennessee State University.

■ ABBREVIATIONS

PLAD Peptoid Library Agar Diffusion
AMP antimicrobial peptide
MIC minimum inhibitory concentration
TD₅₀ toxicity dose 50%
HC₁₀ hemolytic concentration 10%
SR selectivity ratio.

■ REFERENCES

(1) Iyer, K. R.; Revie, N. M.; Fu, C.; Robbins, N.; Cowen, L. E. Treatment Strategies for Cryptococcal Infection: Challenges,

Advances and Future Outlook. *Nat. Rev. Microbiol.* **2021**, *19*, 454–466.

(2) Manley, G. How Sweet It Is! Cell Wall Biogenesis and Polysaccharide Capsule Formation in *Cryptococcus Neoformans*. *Annu. Rev. Microbiol.* **2009**, *63*, 233–247.

(3) Buchanan, K. L.; Murphy, J. W. What Makes *Cryptococcus Neoformans* a Pathogen? *Emerg. Infect. Dis.* **1998**, *4*, 71–83.

(4) Sloan, D. J.; Parris, V. Cryptococcal Meningitis: Epidemiology and Therapeutic Options. *Clin. Epidemiol.* **2014**, *6*, 169–182.

(5) Rajasingham, R.; Smith, R. M.; Park, B. J.; Jarvis, J. N.; Govender, N. P.; Chiller, T. M.; Denning, D. W.; Loyse, A.; Boulware, D. R. Global Burden of Disease of HIV-Associated Cryptococcal Meningitis: An Updated Analysis. *Lancet Infect. Dis.* **2017**, *17*, 873–881.

(6) Merry, M.; Boulware, D. R. Cryptococcal Meningitis Treatment Strategies Affected by the Explosive Cost of Flucytosine in the United States: A Cost-Effectiveness Analysis. *Clin. Infect. Dis.* **2016**, *62*, 1564–1568.

(7) Segal, E.; Elad, D. Special Issue: Treatments for Fungal Infections. *J. Fungi (Basel)* **2018**, *4*, 135.

(8) Perfect, J. R.; Dismukes, W. E.; Dromer, F.; Goldman, D. L.; John, R.; Hamill, R. J.; Harrison, T. S.; Larsen, R. A.; Nguyen, M.; Pappas, P. G.; Powderly, W. G. Guideline for *Cryptococcus*. *Clin. Infect. Dis.* **2010**, *50*, 291–322.

(9) Pappas, P. G. G.; Kauffman, C. A. A.; Andes, D.; Benjamin, D. K.; Calandra, T. F. F.; Edwards, J. E.; Filler, S. G. G.; Fisher, J. F. F.; Kullberg, B. B.-J.; Zeichner, L. O.; Reboli, A. C. C.; Rex, J. H. H.; Walsh, T. J. J.; Sobe, J. D.; Benjamin, D. K., Jr.; Calandra, T. F. F.; Edwards, J. E., Jr.; Filler, S. G. G.; Fisher, J. F. F.; Kullberg, B. B.-J.; Ostrosky-Zeichner, L.; Reboli, A. C. C.; Rex, J. H. H.; Walsh, T. J. J.; Sobel, J. D. Clinical Practice Guidelines for the Management of Candidiasis: 2009 Update by the Infectious Diseases Society of America. *Clin. Infect. Dis.* **2009**, *48*, 503–535.

(10) Vermes, A.; Guchelaar, H. J.; Dankert, J. Flucytosine: A Review of Its Pharmacology, Clinical Indications, Pharmacokinetics, Toxicity and Drug Interactions. *J. Antimicrob. Chemother.* **2000**, *46*, 171–179.

(11) Ben-Ami, R.; Kontoyiannis, D. P. Resistance to Antifungal Drugs. *Infect. Dis. Clin. North Am.* **2021**, *35*, 279–311.

(12) Wiederhold, N. P. Antifungal Resistance: Current Trends and Future Strategies to Combat. *Infect. Drug Resist.* **2017**, *10*, 249–259.

(13) Zafar, H.; Altamirano, S.; Ballou, E. R.; Nielsen, K. A Titanic Drug Resistance Threat in *Cryptococcus Neoformans*. *Curr. Opin. Microbiol.* **2019**, *52*, 158–164.

(14) Nakatsuji, T.; Gallo, R. L. Antimicrobial Peptides: Old Molecules with New Ideas. *J. Invest. Dermatol.* **2012**, *132*, 887–895.

(15) Matejuk, A.; Leng, Q.; Begum, M. D.; Woodle, M. C.; Scaria, P.; Chou, S. T.; Mixson, A. J. Peptide-Based Antifungal Therapies against Emerging Infections. *Drugs Future* **2010**, *35*, 197.

(16) Green, R. M.; Bicker, K. L. Evaluation of Peptoid Mimics of Short, Lipophilic Peptide Antimicrobials. *Int. J. Antimicrob. Agents* **2020**, *56*, No. 106048.

(17) Chongsirawatana, N. P.; Patch, J. A.; Czyzewski, A. M.; Dohm, M. T.; Ivankin, A.; Gidalevitz, D.; Zuckermann, R. N.; Barron, A. E. Peptoids That Mimic the Structure, Function, and Mechanism of Helical Antimicrobial Peptides. *Proc. Natl. Acad. Sci. U. S. A.* **2008**, *105*, 2794.

(18) Gomes Von Borowski, R.; Gnoatto, S. C. B.; Macedo, A. J.; Gillet, R. Promising Antibiofilm Activity of Peptidomimetics. *Front. Microbiol.* **2018**, *9*, 2157.

(19) Mroz, P. A.; Perez-Tilve, D.; Mayer, J. P.; DiMarchi, R. D. Stereochemical Inversion as a Route to Improved Biophysical Properties of Therapeutic Peptides Exemplified by Glucagon. *Commun. Chem.* **2019**, *2*, 2.

(20) Evans, B. J.; King, A. T.; Katsifis, A.; Matesic, L.; Jamie, J. F. Methods to Enhance the Metabolic Stability of Peptide-Based PET Radiopharmaceuticals. *Molecules* **2020**, *25*, 2314.

(21) Mojsoska, B.; Zuckermann, R. N.; Jenssen, H. Structure-Activity Relationship Study of Novel Peptoids That Mimic the

- Structure of Antimicrobial Peptides. *Antimicrob. Agents Chemother.* **2015**, *59*, 4112–4120.
- (22) Spicer, S. K.; Subramani, A.; Aguila, A. L.; Green, R. M.; McClelland, E. E.; Bicker, K. L. Toward a Clinical Antifungal Peptoid: Investigations into the Therapeutic Potential of AEC5. *Biopolymers* **2019**, *110*, No. e23276.
- (23) Goodson, B.; Ehrhardt, A.; Ng, S.; Nuss, J.; Johnson, K.; Giedlin, M.; Yamamoto, R.; Moos, W. H.; Krebber, A.; Ladner, M.; Giacona, M. B.; Vitt, C.; Winter, J. Characterization of Novel Antimicrobial Peptoids. *Antimicrob. Agents Chemother.* **1999**, *43*, 1429–1434.
- (24) Bicker, K. L.; Cobb, S. L. Recent Advances in the Development of Anti-Infective Peptoids. *Chem. Commun.* **2020**, *S6*, 11158–11168.
- (25) Molchanova, N.; Hansen, R. P.; Franzyk, H. Advances in Development of Antimicrobial Peptidomimetics as Potential Drugs. *Molecules* **2017**, *22*, 1430.
- (26) Turkett, J. A.; Bicker, K. L. Evaluating the Effect of Peptoid Lipophilicity on Antimicrobial Potency, Cytotoxicity, and Combinatorial Library Design. *ACS Comb. Sci.* **2017**, *19*, 229–233.
- (27) Kapoor, R.; Wadman, M. W.; Dohm, M. T.; Czyzewski, A. M.; Spormann, A. M.; Barron, A. E. Antimicrobial Peptoids Are Effective against Pseudomonas Aeruginosa Biofilms. *Antimicrob. Agents Chemother.* **2011**, *55*, 3054–3057.
- (28) Patch, J. A.; Barron, A. E. Helical Peptoid Mimics of Magainin-2 Amide. *J. Am. Chem. Soc.* **2003**, *125*, 12092–12093.
- (29) Chongsiriwatana, N. P.; Miller, T. M.; Wetzler, M.; Vakulenko, S.; Karlsson, A. J.; Palecek, S. P.; Mobashery, S.; Barron, A. E. Short Alkylated Peptoid Mimics of Antimicrobial Lipopeptides. *Antimicrob. Agents Chemother.* **2011**, *55*, 417–420.
- (30) Khara, J. S.; Mojsoska, B.; Mukherjee, D.; Langford, P. R.; Robertson, B. D.; Jenssen, H.; Ee, P. L. R.; Newton, S. M. Ultra-Short Antimicrobial Peptoids Show Propensity for Membrane Activity Against Multi-Drug Resistant Mycobacterium Tuberculosis. *Front. Microbiol.* **2020**, *11*, 417.
- (31) Czyzewski, A. M.; Jenssen, H.; Fjell, C. D.; Waldbrook, M.; Chongsiriwatana, N. P.; Yuen, E.; Hancock, R. E. W.; Barron, A. E. In Vivo, In Vitro, and In Silico Characterization of Peptoids as Antimicrobial Agents. *PLoS One* **2016**, *11*, No. e0135961.
- (32) Mojsoska, B.; Carretero, G.; Larsen, S.; Mateiu, R. V.; Jenssen, H. Peptoids Successfully Inhibit the Growth of Gram Negative E. Coli Causing Substantial Membrane Damage. *Sci. Rep.* **2017**, *7*, 42332.
- (33) Kapoor, R.; Eimerman, P. R.; Hardy, J. W.; Cirillo, J. D.; Contag, C. H.; Barron, A. E. Efficacy of Antimicrobial Peptoids against Mycobacterium Tuberculosis. *Antimicrob. Agents Chemother.* **2011**, *55*, 3058–3062.
- (34) Green, R. M.; Bicker, K. L. Development of an Anti-Biofilm Screening Technique Leads to the Discovery of a Peptoid with Efficacy against Candida Albicans. *ACS Infect. Dis.* **2022**, *8*, 310–320.
- (35) Green, R. M.; Bicker, K. L. Discovery and Characterization of a Rapidly Fungicidal and Minimally Toxic Peptoid against Cryptococcus Neoformans. *ACS Med. Chem. Lett.* **2021**, *12*, 1470–1477.
- (36) Middleton, M. P.; Armstrong, S. A.; Bicker, K. L. Improved Potency and Reduced Toxicity of the Antifungal Peptoid AEC5 Through Submonomer Modification. *Bioorg. Med. Chem. Lett.* **2018**, *28*, 3514–3519.
- (37) Corson, A. E.; Armstrong, S. A.; Wright, M. E.; McClelland, E.; Bicker, K. L. Discovery and Characterization of a Peptoid with Antifungal Activity against Cryptococcus Neoformans. *ACS Med. Chem. Lett.* **2016**, *7*, 1139–1144.
- (38) Uchida, M.; McDermott, G.; Wetzler, M.; Le Gros, M. A.; Myllys, M.; Knoechel, C.; Barron, A. E.; Larabell, C. A. Soft X-Ray Tomography of Phenotypic Switching and the Cellular Response to Antifungal Peptoids in Candida Albicans. *Proc. Natl. Acad. Sci. U. S. A.* **2009**, *106*, 19375–19380.
- (39) Luo, Y.; Bolt, H. L.; Eggimann, G. A.; McAuley, D. F.; McMullan, R.; Curran, T.; Zhou, M.; Jahoda, P. C. A. B.; Cobb, S. L.; Lundy, F. T. Peptoid Efficacy against Polymicrobial Biofilms Determined by Using Propidium Monoazide-Modified Quantitative PCR. *ChemBioChem* **2017**, *18*, 111–118.
- (40) Diamond, G.; Molchanova, N.; Herlan, C.; Fortkort, J. A.; Lin, J. S.; Figgins, E.; Bopp, N.; Ryan, L. K.; Chung, D.; Adcock, R. S.; Sherman, M.; Barron, A. E. Potent Antiviral Activity against HSV-1 and SARS-CoV-2 by Antimicrobial Peptoids. *Pharmaceuticals (Basel)* **2021**, *14*, 304.
- (41) Fisher, K. J.; Turkett, J. A.; Corson, A. E.; Bicker, K. L. Peptoid Library Agar Diffusion (PLAD) Assay for the High-Throughput Identification of Antimicrobial Peptoids. *ACS Comb. Sci.* **2016**, *18*, 287–291.
- (42) Archibald, L. K.; Tuohy, M. J.; Wilson, D. A.; Nwanyanwu, O.; Kazembe, P. N.; Tansuphasawadikul, S.; Eampokalap, B.; Chaovanich, A.; Reller, L. B.; Jarvis, W. R.; Hall, G. S.; Procop, G. W. Antifungal Susceptibilities of Cryptococcus Neoformans. *Emerg. Infect. Dis.* **2004**, *10*, 143.
- (43) Cunningham, B. C.; Wells, J. A. High-Resolution Epitope Mapping of HGH-Receptor Interactions by Alanine-Scanning Mutagenesis. *Science* **1989**, *244*, 1081–1085.
- (44) Zuckermann, R. N.; Kerr, J. M.; Kent, S. B. H.; Moosf, W. H. Efficient Method for the Preparation of Peptoids [oligo(N-substituted glycines)] by submonomer solid-phase synthesis. *J. Am. Chem. Soc.* **1992**, *114*, 10646–10647.
- (45) Chemaxon. *MarvinSketch 19.17.0 Was Used for Physicochemical Calculations*; ChemAxon2019, (<https://www.chemaxon.com>).
- (46) Andreev, K.; Martynowycz, M. W.; Huang, M. L.; Kuzmenko, I.; Bu, W.; Kirshenbaum, K.; Gidalevitz, D. Hydrophobic Interactions Modulate Antimicrobial Peptoid Selectivity towards Anionic Lipid Membranes. *Biochim. Biophys. Acta, Biomembr.* **2018**, *1860*, 1414–1423.
- (47) Bolt, H. L.; Eggimann, G. A.; Jahoda, C. A. B.; Zuckermann, R. N.; Sharples, G. J.; Cobb, S. L. Exploring the Links between Peptoid Antibacterial Activity and Toxicity. *Med. Chem. Commun.* **2017**, *8*, 886–896.
- (48) Frederiksen, N.; Hansen, P. R.; Björkling, F.; Franzyk, H. Peptide/Peptoid Hybrid Oligomers: The Influence of Hydrophobicity and Relative Side-Chain Length on Antibacterial Activity and Cell Selectivity. *Molecules* **2019**, *24*, 4429.
- (49) Molchanova, N.; Nielsen, J. E.; Sørensen, K. B.; Prabhala, B. K.; Hansen, P. R.; Lund, R.; Barron, A. E.; Jenssen, H. Halogenation as a Tool to Tune Antimicrobial Activity of Peptoids. *Sci. Rep.* **2020**, *10*, 14805.
- (50) Greco, I.; Molchanova, N.; Holmedal, E.; Jenssen, H.; Hummel, B. D.; Watts, J. L.; Håkansson, J.; Hansen, P. R.; Svenson, J. Correlation between Hemolytic Activity, Cytotoxicity and Systemic in Vivo Toxicity of Synthetic Antimicrobial Peptides. *Sci. Rep.* **2020**, *10*, 13206.